Characterisation of spin coated engineered *Escherichia coli* biofilms using atomic force microscopy

Characterisation of Spin Coated Engineered Escherichia coli Biofilms using Atomic Force Microscopy

Andreas N. Tsoligkas[*], James Bowen[*], Michael Winn[#], Rebecca J.M Goss[#], Tim W. Overton[*], Mark J.H. Simmons[*]

[*]School of Chemical Engineering, University of Birmingham, Edgbaston, Birmingham, B15 2TT, UK
[#]School of Chemistry, University of East Anglia, Norwich, NR4 7TJ, UK

Abstract

The ability of biofilms to withstand chemical and physical extremes gives them the potential to be developed as robust biocatalysts. Critical to this issue is their capacity to withstand the physical environment within a bioreactor; in order to assess this capability knowledge of their surface properties and adhesive strength is required. Novel atomic force microscopy experiments conducted under growth conditions (30 ^{o}C) were used to characterise *Escherichia coli* biofilms, which were generated by a recently developed spin-coating method onto a poly-L-lysine coated glass substrate. High-resolution topographical images were obtained throughout the course of biofilm development, quantifying the tip–cell interaction force during the 10 day maturation process. Strikingly, the adhesion force between the Si AFM tip and the biofilm surface increased from 0.8 nN to 40 nN within 3 days. This was most likely due to the production of extracellular polymer substance (EPS), over the maturation period, which was also observed by electron microscopy. At later stages of maturation, multiple retraction events were also identified corresponding to biofilm surface features thought to be EPS components. The spin coated biofilms were shown to have stronger surface adhesion than an equivalent conventionally grown biofilm on the same glass substrate.

Keywords

Atomic force microscopy, wet mode, biofilm, biotransformations, biocatalyst, cell adhesion

1. Introduction

Biofilm formation is usually undesirable, causing fouling of marine equipment or process plant used in the food, chemical and energy generation industries. Biofilms can also be the source of major human health issues such as lung infections, dental caries and urinary tract infections. This is due to the enhanced ability of bacteria in biofilms to survive nutrient limitation and multiple stresses caused by antibiotics, extremes in temperature or pH and reactive oxygen species.

However, these properties have proved to be exploitable by industry where biofilms used in continuous reactor systems have improved the economics of processes via their increased reactivity and stability. For instance, 29 times more acetic acid has been produced using a biofilm of *Acetobacter aceti* when compared to continuous culture using a jar fermenter [1]. Other applications where biofilm reactors offer greater production than those found in free cells include the production of L-lysine by *Corynebacterium glutamicum* [2], ethanol production using immobilised *Saccharomyces cerevisiae* on ceramic beads [3] and, more recently, the use of a membrane aerated activated sludge biofilm reactor for the degradation of acetonitrile [4]. However, these examples of industrially-used biofilms are based on biofilms which have been formed using strains with a strong propensity to form a biofilm. This process of natural biofilm formation has been extensively studied, whereby bacteria become immobilised onto a support surface in five physiologically and structurally distinctive stages [5]: initial surface attachment; monolayer formation; migration to form multilayer microcolonies; production of an extracellular polymeric substance (EPS) matrix; and finally maturation of the biofilm into a characteristic 3-dimensional architecture. Although this natural process can be exploited technically by industry, it is not economically feasible in large scale technologies because of the length of time required to achieve the desired amount of immobilised biomass per unit volume. This issue has driven research into alternative methods of immobilisation.

In order to produce a biological catalyst, there are three different techniques that can be used to immobilise bacteria: membrane technology; entrapment; and natural adsorption for biofilm formation. Membrane technology, where the cells are grown or forced into the pores, has several major industrial applications for the degradation of phenol [6] and chlorophenols [7]. However, the cost of manufacture can limit the applications for larger scales. Similarly, entrapment requires specialised chemicals such as bioglues, which can prove too expensive. Apart from the membrane bioreactors, there are several other types of biofilm reactors such as the fluidised bed biofilm reactor (FBBR, [8-9]) and packed bed reactor [10]. Both types of reactors have been proven to offer a high biomass holdup which enables high liquid throughputs and high residence time using the natural cell immobilisation and have been found to be successful for both aerobic and anaerobic cultures. However, the biomass growth on these types of reactors can be time consuming with an unpredictable pattern of biofilm formation on the surfaces.

In a previous paper, a novel route for the immobilisation of bacteria into catalytic biofilms using spin-coating is described, using a technique more commonly employed for the immobilisation of inorganic catalyst onto surfaces [11]. Spin coating examples can be found in waste water treatment using photocatalysis [12] (Kim *et al.,* 2009), where TiO_2 particles have been successfully deposited onto a glass substrate. Other applications include the rapid deposition of nanoparticles for fabrication of nanostructures with typical applications in the optoelectronic industry [13] including the deposition of precious metals such as Pt for the manufacture of solar cells [14]. The principal benefit of using this technique to generate spin coated engineered biocatalysts (SCEBs) is that the lengthy processes of initial surface attachment and monolayer formation are overcome, while the maturation of SCEB on minimal media will allow generation of EPS and the formation of a physically strong three dimensional biofilm. The resultant SCEBs have potential wide ranging applications within the chemical and pharmaceutical industries [11]

In this paper, we expand upon our novel biocatalyst generation methodology by describing new methods to analyse catalytic biofilms. Atomic force microscopy (AFM) is a technique based on measuring intermolecular forces between a sharp tip and the surface of a sample with a reported lateral resolution up to 1-3 nm [15]. In this study, AFM is employed to primarily determine the adhesion of the bacterial cells when probed with the AFM tip. AFM has been previously been used to examine biofilms both in terms of adhesion measurements and snap-off events from the AFM tip, which have been used to characterise biomolecules on cell surfaces, since each biomolecule has distinctive adhesion behaviour [16]. AFM measurements of interaction forces for corrosive biofilms on metal surfaces have found that the forces are twice as high on the cell – cell interface compared with the cell- metal

surface interface [17]. More recently, the adhesion forces between Gram negative with Gram positive bacterial biofilms have been compared [18], with the interesting result that Gram positive bacteria are densely packed with EPS, possessing high adhesion forces and short distance snap-off events, compared to the smaller adhesion forces and less dense packing found in Gram negative bacterial biofilms. Statistical analyses of *Staphylococcus epidermis* adhesion forces as measured by AFM, employing single bacterial cells immobilised at the cantilever apex, have offered insight into the mechanisms of bacterial adhesion, encompassing both long-range and short-range forces [19].

To our knowledge, adhesion force-distance and global force measurements, important to qualitatively and quantitatively characterise SCEBs, have not been investigated. A recent study examining the physicochemical changes in *Xylella fastidiosa* biofilms employed AFM and electron microscopy, concluding that that rough, hydrophobic surfaces promote biofilm formation [20]. In this paper, we use wet mode AFM method in order to quantify the adhesion forces found in SCEBs throughout the maturation period. Apart from the force measurements, we reveal the snap-off events that take place over a 10 day period. We show that the measured forces, non linear retraction of tip and global forces of SCEBs are dependent on maturation period and SCEBs are more adhesive when compared with the natural biofilm. These data, whilst of interest in characterising the morphology and maturation of the novel SCEBs, also provide vital information in terms of robustness of the biocatalyst, in developing the industrial application of the concept.

2. Materials and methods

2.1 Media and strains

A sample of *E. coli* pre-transformed with pSTB7, a pBR322-based plasmid containing the *Salmonella enterica* serovar Typhimurium TB1533 *trpA* and *trpB* genes and encoding ampicillin resistance [21], was purchased from the American Type Culture Collection (ATCC 37845, deposited by E. W. Miles). *E. coli* K-12 strain PHL644 (MC4100 *malA-kan ompR234*) was kindly provided for use in this study by O. Vidal [22]. This strain produces a thick biofilm as a consequence of a point mutation in the regulatory protein OmpR, resulting in the overproduction of adhesive curli fibres.

E. coli PHL644 was transformed with pSTB7 using the heat-shock method. Transformants were selected on LB-agar (10 g L^{-1} tryptone, 5 g L^{-1} yeast extract, 10 g L^{-1} NaCl, 15 g L^{-1} Bacteriological Agar) supplemented with ampicillin (100 µg mL^{-1}). Transformants were grown in Luria-Bertani (LB) broth (10 g L^{-1} tryptone, 5 g L^{-1} yeast extract, 10 g L^{-1} NaCl) supplemented with ampicillin (100 µg L^{-1}) or Half-Luria-Bertani (½ LB) broth (5 g L^{-1} tryptone, 2.5 g L^{-1} yeast extract, 5 g L^{-1} NaCl) supplemented with ampicillin (100 µg mL^{-1}). Surface-adhered biofilms were maturated and curli expression was promoted in M63 medium (100 mM KH_2PO_4, 15 mM $(NH_4)_2SO_4$, 0.8 mM $MgSO_4.7H_2O$, 9 mM $FeSO_4.2H_2O$, 17 mM K-succinate, 1 mM glucose, adjusted to pH 7.0) with the addition of ampicillin (100 µg mL^{-1}).

2.2 Biofilm generation and maturation: preparation of glass slides with poly–L–lysine (PLL), as substrate for the immobilisation of the spin coated and natural biofilm.

All biofilms in this study were investigated in the form of thin layers on glass microscope slides (75 mm by 25 mm, VMR). Prior to biofilm formation, glass slides were coated with approximately 4 mL of 0.1 % (w/v) PLL in water (Sigma), which was then dried overnight in an oven at 60 °C. 10 µL of a culture of *E. coli* PHL644 transformed with pSTB7 was streaked onto an agar plate supplemented with 100 µg mL^{-1} ampicillin and incubated at 37 °C for 14 hours. Single colonies were picked and used to inoculate 200 mL of ½×LB supplemented with ampicillin (100 µg mL^{-1}). The culture was incubated in an orbital shaker at 30 °C, 180 rpm with a throw of 19 mm for 16 hours.

Following incubation, cultures were transferred aseptically into sterile 750 mL polypropylene centrifuge bottles (Beckman Coulter UK Ltd.) containing the PLL-coated glass slides supported on a bed of glass beads (200 g, soda-glass beads, 4 mm diameter) to provide a flat surface to prevent cracking during centrifugation and were centrifuged at 1851 g for 10 minutes in a centrifuge fitted with a swinging bucket rotor. After centrifugation, the glass slides coated with bacteria were gently placed into 500 mL sterilised wide necked Erlenmyer flasks (Fisher Scientific) containing 70mL of M63 medium supplemented with ampicillin (100 µg mL^{-1}). The spin coated biofilms were incubated in an orbital shaker incubator at 30 °C, 70 rpm with a throw of 19 mm (the low speed was selected to minimise bacteria shearing from the biofilm) for a maturation period of 7 days. Natural biofilms were generated by harvesting the 16-hour cultures by centrifugation (1851 g for 15 mins), and resuspending the bacteria in 70 mL of M63 medium in a 500 mL wide necked Erlenmyer flask into which a PLL coated glass slide was introduced. The slide was incubated for 7 days at 30 °C and 150 rpm, in an orbital shaker incubator with a throw of 19 mm.

2.3 Biofilm analysis: AFM and force analysis

The biofilm-coated glass slides were removed from the media after 3-10 days of growth and a 7 × 7 mm area was carefully sliced and firmly secured in a BioCell (JPK, Germany) containing 1 mL of M63 medium in order to perform the wet mode experiments at 30 °C. The temperature in the BioCell was allowed to equilibrate at 30 °C and then mounted in a NanoWizard II AFM (JPK, Germany) incorporating a CellHesion module (JPK, Germany), providing a lateral scan range of 100 µm × 100 µm, and a vertical range of 90 µm. The wet mode experiments in M63 solution preserves the biofilm interactions and attachment and provides accurate force measurements compared to dry mode [23]. A minimum of 10 force measurements were collected on each of five different biofilm regions on the same sample, each region covering an area of 100 µm × 100 µm, affording a typical total of >100 force measurements. Measurements were performed on three separately grown biofilms and the results collated, giving somewhere in the region of 300-500 force measurements for each day of biofilm maturation. For each day of maturation, all of the recorded force measurements are summed to produce an overall global force distribution and examined using the Gaussian function in order to obtain a mean and standard deviation for each day of maturation. The Gaussian function, $f(x)$, is defined in Eq. 1 as:

$$f(x) = ae^{-\frac{(x-b)^2}{2c^2}} \quad (1)$$

where, a is a constant, b is the mean force, c^2 is the variance, and x is the force.

During measurements, the cantilever tip was brought into contact with the biofilm surface under a compressive load of 10 nN for a period of < 1 s. Upon retraction of the AFM cantilever, the peak vertical deflection was converted to a peak force via multiplication of the measured deflection by the nominal cantilever spring constant of 0.9 N m^{-1}. In this study, microfabricated rectangular Si cantilevers (of 450 μm length) were used with pyramidal oxide sharpened tips of 10 nm nominal radius of curvature (MikroMasch, Estonia), and a scan velocity of 5 µm s^{-1} was employed throughout.

2.4 Environmental Scanning Electron Microscopy (ESEM)

Biofilm samples were also examined using ESEM using standard methods to treat the biofilm prior to imaging [24]. The biofilm samples were immersed in 2.5% glutaraldehyde for 24 h in order to preserve the structure of living tissue with no alternation from the living state. After the primary fixation with glutaraldehyde, the biofilm samples were dehydrated for 15 mins using aqueous solutions of ethanol of increasing concentration (50%, 70%, 90%, 100% ethanol and 100% dried ethanol). The dehydration was applied twice for each concentration. After fixation and rinsing, the samples were critical point dried using a critical point dryer (Agar Scientific, UK) and then mounted onto microscope stubs for Pt coating using an Emscope SC 500 sputter coater (Emscope, Ashford, UK), and examined using a XL-30 FEG ESEM (Cambridge Instruments, Cambridge, UK).

3. Results and Discussion

3.1 Formation of SCEBs

The regulation of biofilm synthesis in *E. coli* is complex and only partially understood [5]. It is known that the synthesis of the various protein and non-proteinaceous determinants of biofilm structure and function is regulated in response to multiple environmental stimuli including osmolarity, temperature, pH, oxygen and growth rate via a complex regulatory network [5]. The present work is focused on *E. coli* K-12 strain PHL644 [24], which readily generates curli and displays a hyperadhesive phenotype. Curli are extracellular protein fibres that have been shown to mediate adhesion, colonisation, and biofilm formation [25-27]. This strain carries a mutation in the osmolarity-responsive response regulator OmpR (*ompR234*) which leads to increased activation of *csgD* expression. The *csgD* gene product is a transcriptional regulator that activates expression of the curlin structural genes *csgBA*, thus increasing curli synthesis. CsgD is also thought to regulate the synthesis of cellulose, a component of EPS, via c-di-GMP signalling [28]. Even in this strain, growth and maturation conditions were designed to optimise biofilm formation.

E. coli PHL644 was grown to stationary phase in ½×LB medium, growth conditions allowing enhanced biofilm formation due to increased curli expression [25]. Similarly, maturation conditions were defined to allow rapid biofilm development. Initial experiments investigating maturation of natural *E. coli* PHL644 biofilms in M63 (minimal) and 1× and ½×LB (rich) media at 30 °C and 37 °C found that the lower temperature and minimal medium gave higher surface coverage and enhanced development of three-dimensional biofilm structure, as previously suggested by [25]. Spin-coating *E. coli* onto the solid substrate removed the need for initial attachment and monolayer formation, but the growth conditions chosen were designed to promoter later stages of biofilm development.

3.2 Development and maturation of SCEBs: electron microscopy

Stationary phase *E. coli* PHL644 were immobilised onto glass slides using spin-coating and allowed to mature for 10 days in M63 medium. The development of the SCEB during the maturation process was investigated using a variety of techniques. In general, spin-coated *E. coli* PHL644 was able to form a mature biofilm at Day 6 of maturation. Figs 1-5 show typical ESEM images of SCEBs at Days 3-7 of maturation respectively, over a range of magnifications suitable for illustrating the micro- and nanoscale detail of the biofilm, as well as the gross surface morphology.

To illustrate the change in biofilm morphology with increasing maturation time, a comparison can be made between the Day 3 SCEB and the Day 6 SCEB. The surface morphology of Day 3 SCEB (Fig. 1a) is significantly different to Day 6 SCEB (Fig. 4a). The Day 6 SCEB appears rougher, with peaks and valleys having formed. Shallow pores, mushroom-shape microcolonies and possibly interconnected microchannels appear to have formed between Day 3 and Day 6, as can be seen by comparing Fig. 1b and Fig. 4b. The shallow pores are believed to be a part of a bigger network of microchannels that are formed to allow nutrients to flow in and out the biofilm. A comparison of Fig. 1c and Fig. 4c reveals the marked difference in the levels of EPS production between Day 3 and Day 6. EPS production is highly localised to a few bacteria on Day 3, but is much more extensive by Day 6. As reported previously [29], the EPS contributes towards the mechanical stability of biofilms, enabling them to withstand considerable shear forces. It is worth noting that curli and other proteinaceous biofilm determinants will also contribute to SCEB strength and the complex three dimensional structure of the biofilm. From examination of Figs 1-5, particularly at high magnifications, it can be seen that SCEBs on Day 3-5 exhibit small amounts of EPS production, whereas SCEBs on Day 6-7 exhibit extensive amounts of EPS production.

To determine whether natural *E. coli* PHL644 biofilms can form a similar structure to the SCEBs, ESEM has previously been employed to compare Day 7 natural biofilm and Day 7 SCEBs [11]. The natural biofilm was shown to have formed a sparse monolayer by Day 7, whereas the SCEB had an extensive three dimensional morphology with EPS throughout (Fig. 5c). Similar to the Day 6 SCEB shown in Fig. 4, shallow pores and channels had formed by Day 7. In comparison, the natural biofilm was unable to mature into a fully developed biofilm with EPS and flow channels, which are basic biofilm characteristics. These data indicate that spin coating helps to overcome the long period of initial attachment of bacteria to the surface, as described in further detail in [11].

3.3 Force characterisation

Several investigators have used methods such as chemical fixation/dehydration or wet mode, in which samples are completely immersed in a liquid medium, to improve AFM imaging of microbial cells. A resolution of 2 nm has been reached using LiCl treatment to chemically fix *Lactobacillus helveticus* [15]. Although pre-treatment improves the image resolution, there is a question as to whether fixation procedures interfere with the force measurements as has been shown previously [30-32]. To provide realistic global force measurements on viable biofilms, wet mode experiments were employed in this study. In addition, the AFM cantilever and biofilm substrate were completely immersed in M63 medium to avoid the inference of capillary forces between the tip and wet bacterial surfaces. Fig. 6 shows the distribution of peak forces and fitted Gaussian function, as described in §2.3, whilst Fig. 7 shows the mean peak forces and standard distributions as obtained from the Gaussian analysis for SCEBs matured for between 3-10 days. Although this study is focused upon gaining overall insight into SCEB evolution and adhesive strength, polyprotein stretching and snap-off events were observed in the AFM force-distance data [32], and the frequency of such events was found to increase with increasing biofilm maturation. Table 1 lists the typical number of snap-off events as a for each day of SCEB maturation, while Fig. 8 shows a number of typical retraction events for SCEBs matured for between 3-10 days. Finally, the distribution of forces measured for the natural biofilm after 7 days of maturation are shown in Fig. 9, along with a number of typical force measurements (inset).

3.3.1 Global measurements

The distributions of peak forces presented in Fig. 6 show that there is a significant change between Day 5 and Day 6 in the SCEB surface properties. Fig. 7 shows that the mean peak adhesion force increased from approximately 1 nN on Day 3-5, with no significant difference between these days, to a force typically in the region 30-60 nN on Day 6-10, with a large distribution of forces measured on each of these days. These results compare well with the increase in the typical number of snap-off events, shown in Table 1, whereby Day 5-7 appears to be a transition period. On Day 3-5 there were typically 1-2 snap-off events during AFM tip retraction, whilst on Day 6 there were typically 3-7 snap-off events. On Day 7-10 there were 5-10 or an even greater number of snap-off events. These results, in conjunction with the ESEM images discussed in §3.2, demonstrate that there are significant changes in the surface properties of the *E. coli* SCEB during the maturation process that serve to increase the adhesive properties of the SCEB once 5 days of maturation have passed. The non-uniform distribution of forces shows the biological and chemical heterogeneity of the SCEB surface. The dramatic increase in adhesive force is likely due to the increase in EPS production over time, as observed by ESEM. Previous studies on the maturation of biofilm formed using *E. coli* strain 0157:117 ATCC 43894 have shown 10-, 14- and 53-fold increases in the intensity of stained EPS after 1, 3 and 5 days maturation [35], which is consistent with the qualitative observations made using ESEM in this study. Secondly, even though the amount of EPS increases with biofilm age, EPS is highly heterogenous in terms of chemical structure, being composed of several distinct polysaccharides and other components [36] and in terms of spatial distribution of material throughout the biofilm. In addition, both composition and distribution change over time, the biofilm being a highly dynamic system.

3.3.2 Individual measurements

By probing individual cells from the early stages of SCEB formation to after 10 days of maturation, it was possible to detect retraction events corresponding to surface macromolecules. The existing Si cantilevers used in this study are not capable of identifying specific molecules, however the resulting force -distance data shown in Fig. 8 reveal that retraction events occur between the tip and cell surface on all days of maturation. On Day 3 (Fig. 8a) a single deflection event is typically shown, suggesting that the tip was in contact with the cell itself and not with any surface macromolecule. On Day 4 onwards, sudden deflections were identified, with single and multiple examples of such events clearly visible in Figs 8b, 8c and 8d. The frequency of these retraction events increases as the SCEB matures, as summarised in Table 1. Similar multiple stepped events have been reported using AFM to map the positions of polysaccharides on the surface of viable yeast cells [16] and in the study of glucan polymers in *Streptococcus mutans* [37]. It could be postulated that these retraction events are either unfolding of polysaccharide moieties [37-38], unfolding of proteins contacted by the AFM tip [39], or successive release of multiple molecules connecting the biofilm and AFM tip [16,37]. For SCEBs matured for 7 days and beyond, there are multiple retraction events over a range of magnitudes, often with the initial event having a magnitude less than the following events. This phenomenon, with an initial small deflection followed by a larger one, has previously been observed for mannan polymers [16]. Given the extension distances measured during the multiple retraction events, which are typically on the order of 200 nm to 1 µm or greater, and the heterogenous nature of the

retraction events, it is most likely that these force spectra reflect interactions between the AFM cantilever tip and multiple strands of EPS, which is itself a complex mixture of different polymeric substances, including cellulose, PGA, colonic acid, and protein strands.

3.4 AFM comparison of SCEBs and Natural Biofilms

Previous work using ESEM revealed that natural biofilms formed on glass slides comprised a single cell layer [11], nonetheless the natural biofilm was allowed to mature for 7 days and compared with the corresponding Day 7 SCEB. Fig. 9 shows that the measured force-distance data resemble that measured for SCEBs on Day 3 and Day 4. No polyprotein extension events are observed, which in turn suggests little or no formation of EPS, which has been previously confirmed by ESEM [11]. The overall force distribution shown in Fig. 9 was calculated based on three samples and suggests an average adhesion force of 2.2 nN, which is much lower than the Day 7 SCEB. The standard deviation and the adhesion forces for the SCEBs increase dramatically on Day 6 compared to the natural biofilm. The standard deviation of the natural biofilm was 0.7 nN compared to 12 nN for the Day 7 SCEB, suggesting that natural biofilms, formed under the same conditions with SCEBs, are unable to produce complex EPS structures.

4. Conclusion

Atomic force microscopy performed using an environmental cell has allowed interrogation of the surface of SCEBs in a condition equivalent to the living state. The AFM experiments showed that the mean peak adhesive force of the biofilm greatly increased from < 1 nN to ~ 40 nN between days 5 and 6 of maturation, correlating with generation of EPS over this period as observed using ESEM. The SCEBs were considerably stronger and matured more rapidly than 'natural' biofilm grown using the same strain over the same period; natural biofilm development after 7 days of maturation resulted in a monolayer of bacteria (peak adhesive force ~ 1 nN). Examination of individual force-distance curves from the AFM revealed multiple retraction or 'snap-off' events after 6 days of maturation, corresponding to the formation of EPS. These events may be attributed to interactions between the probe tip and the EPS. Further work into the nature of the origin of these interactions should employ chemically modified tips and include a more in-depth statistical analysis of the measured forces, work of adhesion, and polyprotein pulling events.

Acknowledgements
ANT, MJS, MW and RJMG acknowledge the financial support from EPSRC Chemistry-Chemical Engineering Discipline Hopping Awards (Grants EP/E000843/1 and EP/E000894/1). The AFM used in this research was obtained through Birmingham Science City: Innovative Uses for Advanced Materials in the Modern World (West Midlands Centre for Advanced Materials Project 2), with support from Advantage West Midlands (AWM) and part funded by the European Regional Development Fund (ERDF).

References

1. K. Toda, T. Asakura, Biotechnol. Lett. 16 (1992) 617.
2. S.G. Velizarov, E. I. Rainina, A. P. Sinitsyn, S. D. Varfolomeyev, V. I. Lozinsky, A. L. Zubov, Biotechnol. Lett. 14 (1992) 291.
3. B. Demuyakor, Y. Ohta, Appl. Microbiol. Biot. 36 (1992) 717.
4. T. Li, R. Bai, D.G. Ohandja, J. Liu, Biodegradation 20 (2009) 569.
5. T. Romeo, Bacterial Biofilms, Springer-Verlag, Berlin, 2008.
6. C.R. Woolard, R.D. Irvine, Water Environ. Res. 66 (1994) 230.
7. A. Wobus, S. Ulrich, I. Roske, Water Sci. Technol., 32 (1995) 205.
8. W.K. Shieh, J.D. Keenan, Adv. Biochem. Biotechnol. 33 (1986) 131.
9. K. Kryst D.G. Karamanev, Ind. Eng. Chem. Res. 40 (2001) 5436.
10. A. Gomez – De Jesus, J. Romano - Baez, L. Leyva - Amezcua, C. Juarez - Ramirez, N. Ruizordaz, J. Galindez – Mayer, J. Hazard. Mater. 161 (2009) 1140.
11. A.N. Tsoligkas, M. Winn, J. Bowen, T.W. Overton, M.J.H. Simmons, R.J.M. Goss, ChemBioChem 12 (2011), 1391.
12. C. Kim, J.T. Kim, K.S. Kim, S. Jeong, H.Y. Kim, Y.S. Han, Electrochim. Acta 54 (2009) 5715.
13. S. Maenosono, T. Okubo, Y. Yamaguchi , J. Nanopart. Res. 5 (2003) 5.
14. M.S. Kang, J.W. Lee, B.C. Shin, United States Patent Application 20090173920, 2009.
15. I. Y. Sokolov, M. Firtel, G. S. Henderson, J. Vac. Sci. Technol. 14 (1996) 674.
16. M. Gad, A. Itoh, A. Ikai, Cell Biol. Int. 21 (1997) 697.
17. L.C. Xu, K.Y. Chan, H.H.P. Fang, Mater. Charact. 48 (2002) 195.
18. C.B. Volle, M.A. Ferguson, K.E. Aidala, E.M. Spain, M.E. Núňez, Colloid. Surface. B 67 (2007) 32.
19. Y. Chen, H.J. Busscher, H.C van der Mei, W. Norde, Appl. Environ. Microbiol. 77 (2011) 5065.
20. G.S. Lorite, C.M. Rodrigues, A.A. de Souza, C. Kranz, B. Mizaikoff, M.A. Cotta, J. Colloid Interface Sci. 359 (2011) 289.
21. H. Kawasaki, R. Bauerle, G. Zon, S.A Ahmed, E.W. Miles, J. Biol. Chem. 262 (1987), 10678.
22. O. Vidal, R. Longin, C. Prigent-Combaret, C. Dorel, M. Hooreman P. Lejeune, J. Bacteriol. 180 (1998) 2442.
23. F. Ahimou, M.J. Semmens, P.J. Novak, G. Haugstad (2007) Appl. Environ. Microb, 73 (2007) 2897.
24. J.J. Bozzala, L.D. Russell, Electron Microscopy, Jones & Bartlett Publishers, Sudbury MA, 1992.
25. C. Prigent-Combaret, E. Brombacher, O. Vidal, A. Ambert, P. Lejeune, P. Landini, C. Dorel, (2001) J. Bacteriol. 183 (2001) 7213.
26. R. Houdt, C.W. Michiels Res. Microbiol 156 (2005) 626–633.
27. Z. Saldaña, J. Xicohtencatl-Cortes, F. Avelino, A.D. Phillips, J.B. Kaper, J.L Puente, J.A Girón. Environ. Microbiol. 11 (2009) 992.
28. E. Brombacher, C. Dorel, A.J.B Zehnder, P. Landini, Microbiol-SGM 149 (2003) 2847.
29. C. Mayer, R. Moritz, C. Kirschner, W. Borchard, R. Maibaum, J. Wingender, H.C Flemming, Int. J. Biol. Macromol. 26 (1999) 3.
30. A. Razatos, Y-L Ong, Y-L., M.M. Sharma, G. Georgiou, G, *Proc. Natl. Acad. Sci. USA* 95 (1998) 11059.
31. A. Razatos, Y-L Ong, Y-L., M.M. Sharma, G. Georgiou, G, 1998. *J. Biomater. Sci. Polym. Ed***.** 9 (1998)**.** 1361.
32. P.E. Marszalek, H. Lu, H. Li, M. Carrion-Vazquez, A.F. Oberhauser, K. Schulten, J.M. Fernandez, Nature 402 (1999) 100.
33. I.D. Auerbach, C. Sorensen, H. G. Hansma, P. A. Holden, J. Bacteriol. 182 (2000) 3809.
34. A. Mendez-Vilas, A.M. Gallardo-Moreno, M.L. Gonzalez-Martin, R. Calzado-Montero, M.J. Nuevo, J.M. Bruque, C. Perez-Giraldo, Appl. Surf. Sci. 238 (2004) 18.
35. J. S. Lim, K. M. Lee, S. H. Kim, S. W. Nam, Y. J .Oh, H. S. Yun, W. Jo, S. Oh, S. Kim, S. Park, Bull. Korean Chem. Soc. 29 (2008) 2114.
36. I. Sutherland, Microbiol. 147 (2001) 3.
37. S.E. Cross, J. Kreth, L. Zhu, R. Sullivan, WY Shi, F-X, Qi, J.K. Gimzewski, Microbiol.-SGM 153 (2007) 3124.
38. G., Francius, S. Lebeer, D. Alsteens, L. Wildling, H.J. Gruber, P. Hols, S. De Keersmaecker J. Vanderleyden, Y.F. Dufrene, ACS Nano., 2 (2008) 1921.
39. T.E. Fisher, P.E. Marszalek, J.M. Fernandez, Nature Struct. Biol. 7 (2000), 719.

Tables

Table 1. Typical number of polyprotein snap-off events as a function of maturation time. A minimum of 30 measurements were analysed from AFM data acquired for each day, across three different samples.

Maturation time (days)	Typical number of snap-off events (-)
3	1-2
4	1-2
5	1-2
6	3-7
7	5-10
8	5-10
9	6-12
10	> 12

List of Figures

Figure 1. ESEM Images of PHL644 (MC4100 *malA-kan ompR234*) growth using spin coat technology for a Day 3 SCEB at magnifications of a) 682×, b) 2730×, c) 10920×.

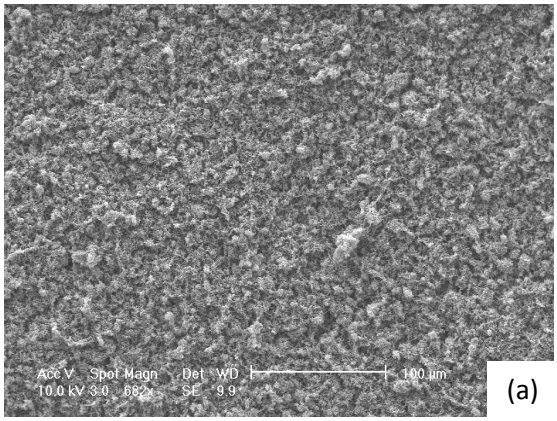

(a)

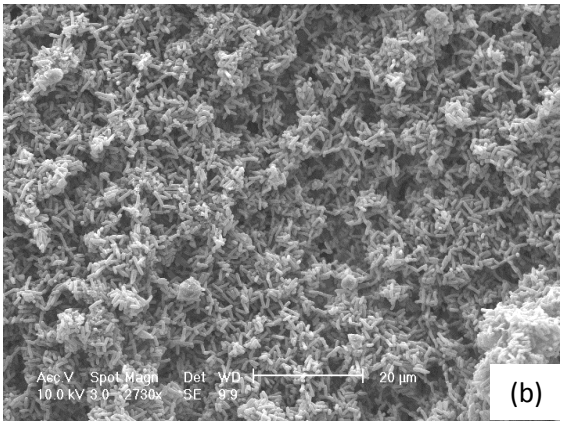

(b)

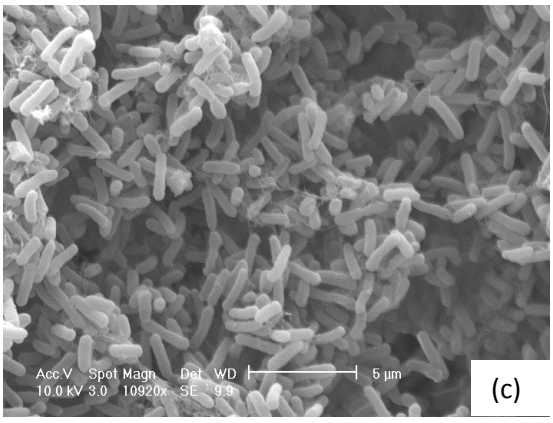

(c)

Figure 2. ESEM Images of PHL644 (MC4100 *malA-kan ompR234*) growth using spin coat technology for a Day 4 SCEB at magnifications of a) 2738×, b) 10951×, c) 43805×.

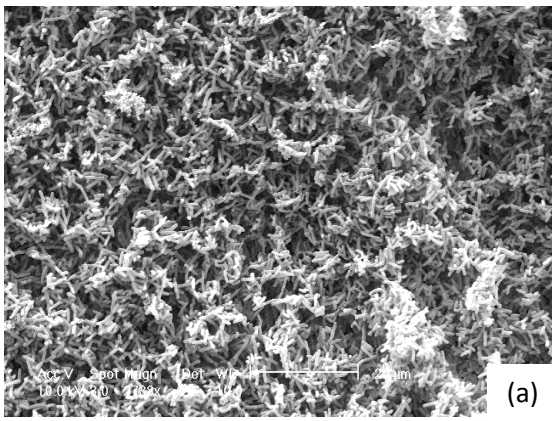

(a)

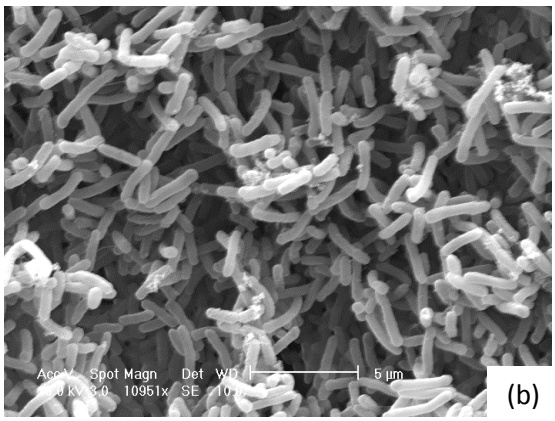

(b)

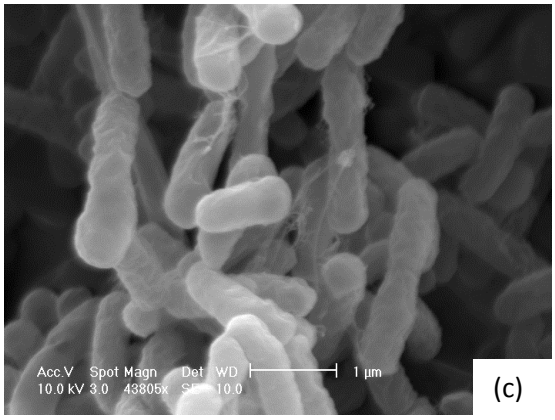

(c)

Figure 3. ESEM Images of PHL644 (MC4100 *malA-kan ompR234*) growth using spin coat technology for a Day 5 SCEB at magnifications of a) 2737×, b) 10914×, c) 21828×.

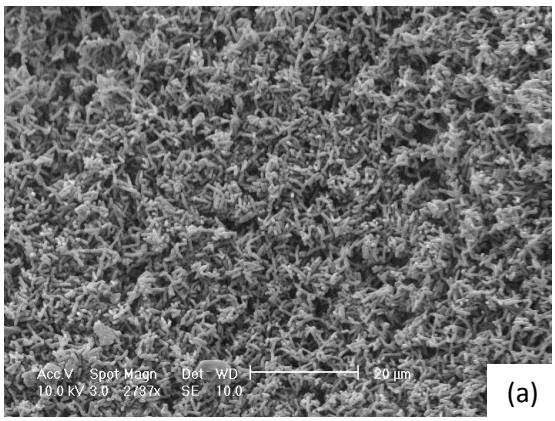

(a)

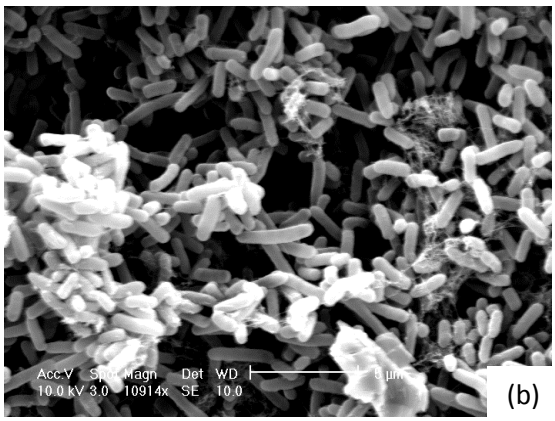

(b)

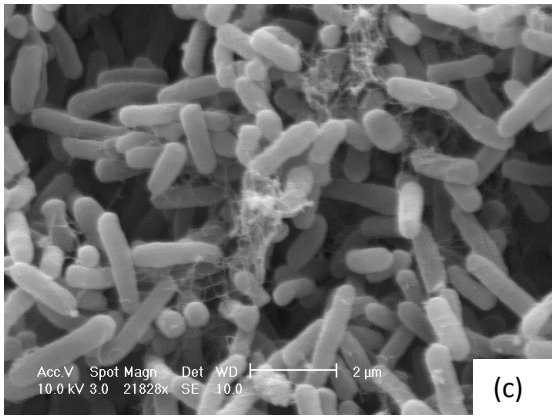

(c)

Figure 4. ESEM Images of PHL644 (MC4100 *malA-kan ompR234*) growth using spin coat technology for a Day 6 SCEB at magnifications of a) 488×, b) 1953×, c) 15625×.

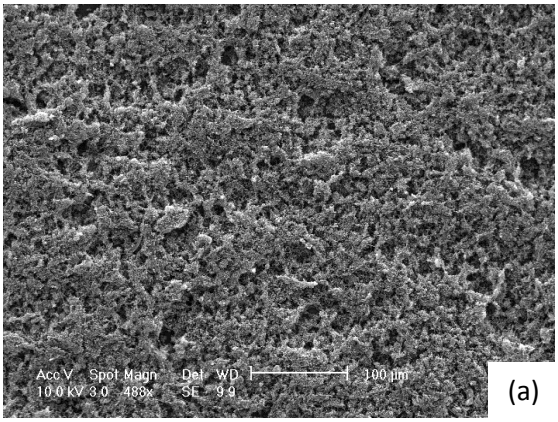

(a)

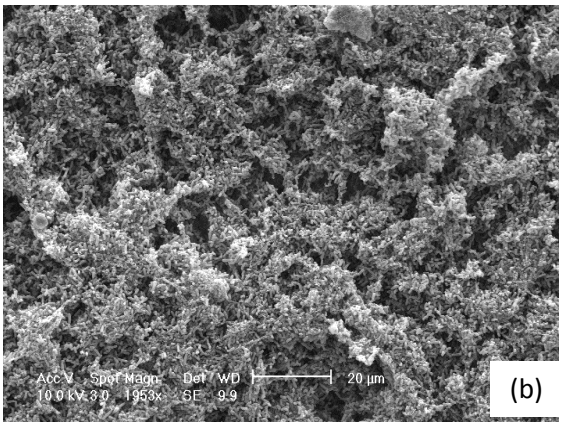

(b)

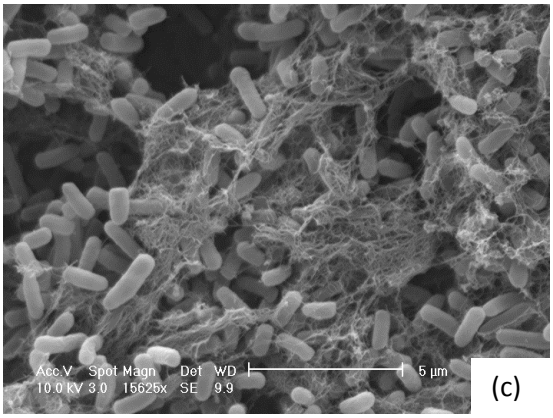

(c)

Figure 5. ESEM Images of PHL644 (MC4100 *malA-kan ompR234*) growth using spin coat technology for a Day 7 SCEB at magnifications of a) 1200×, b) 2401×, c) 9604×.

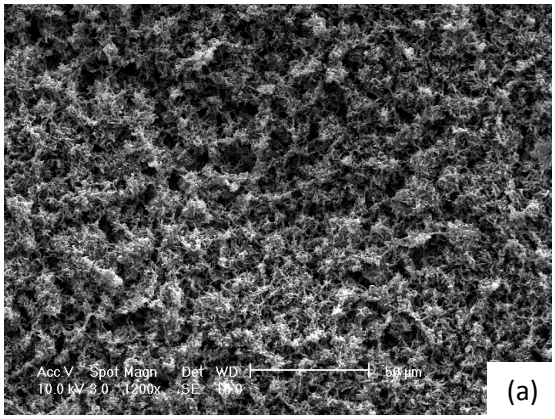

(a)

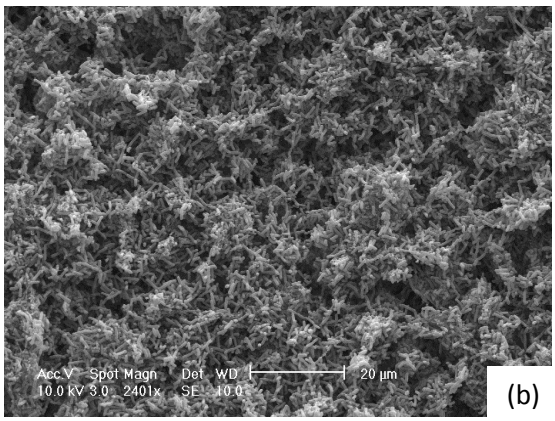

(b)

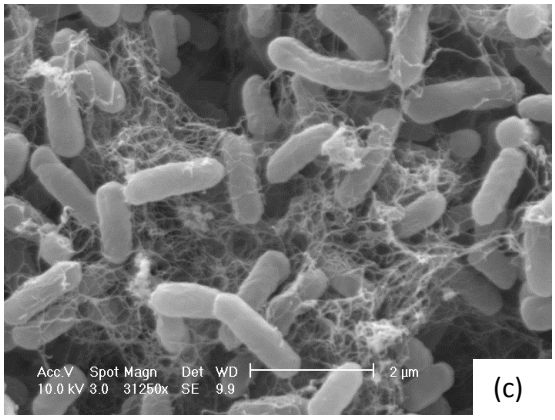

(c)

Figure 6. Distribution of peak forces measured using AFM for SCEBs on a) Day 3, b) Day 4 B, c) Day 5, d) Day 6, e) Day 7, f) Day 8, g) Day 9, h) Day 10. A minimum of 300 measurements were performed on each day, on three different samples.

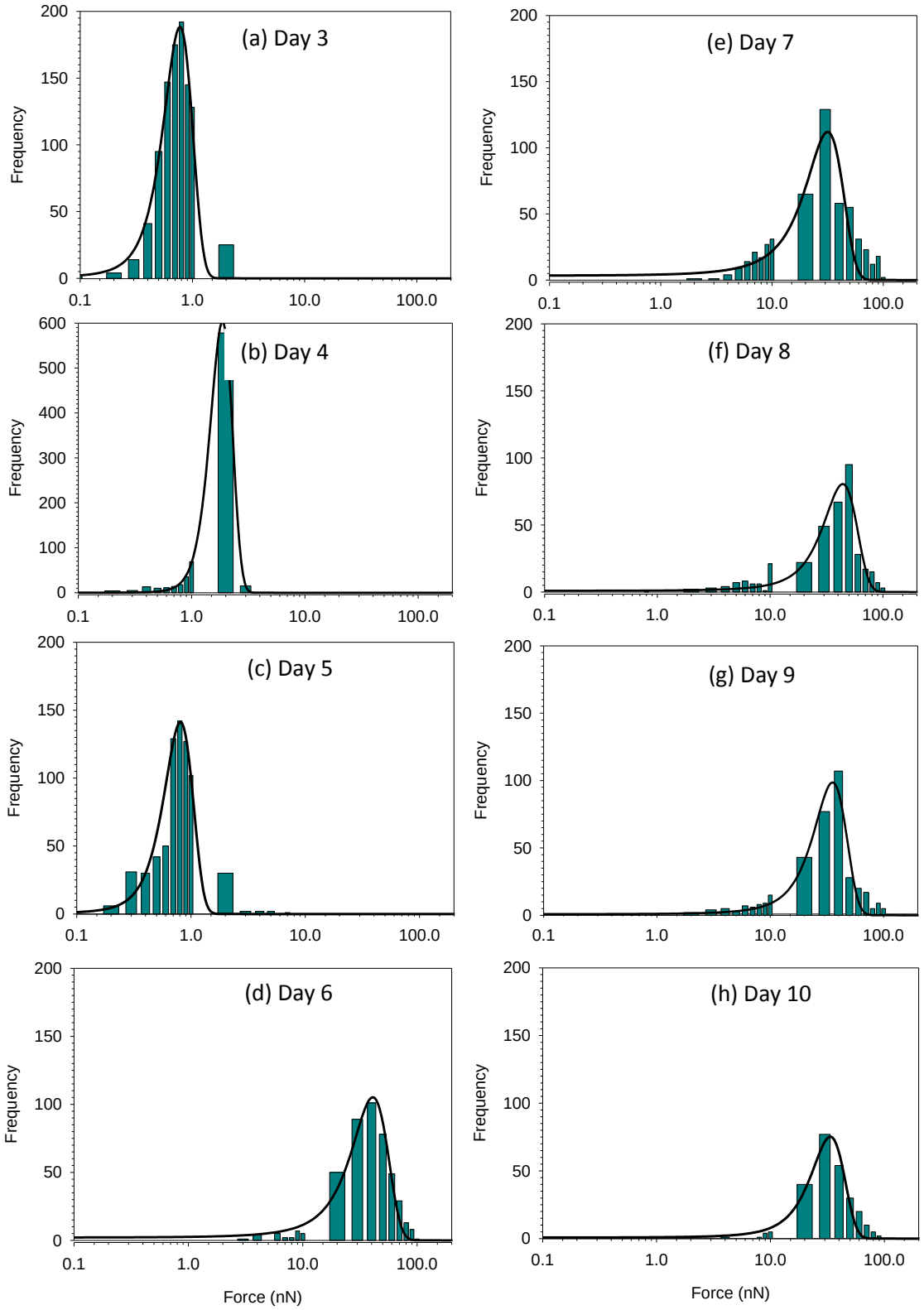

Figure 7. Mean peak forces and standard deviations calculated using a Gaussian analysis of measured AFM data for SCEBs matured for between 3-10 days. A minimum of 300 measurements were performed on each day, on three different samples.

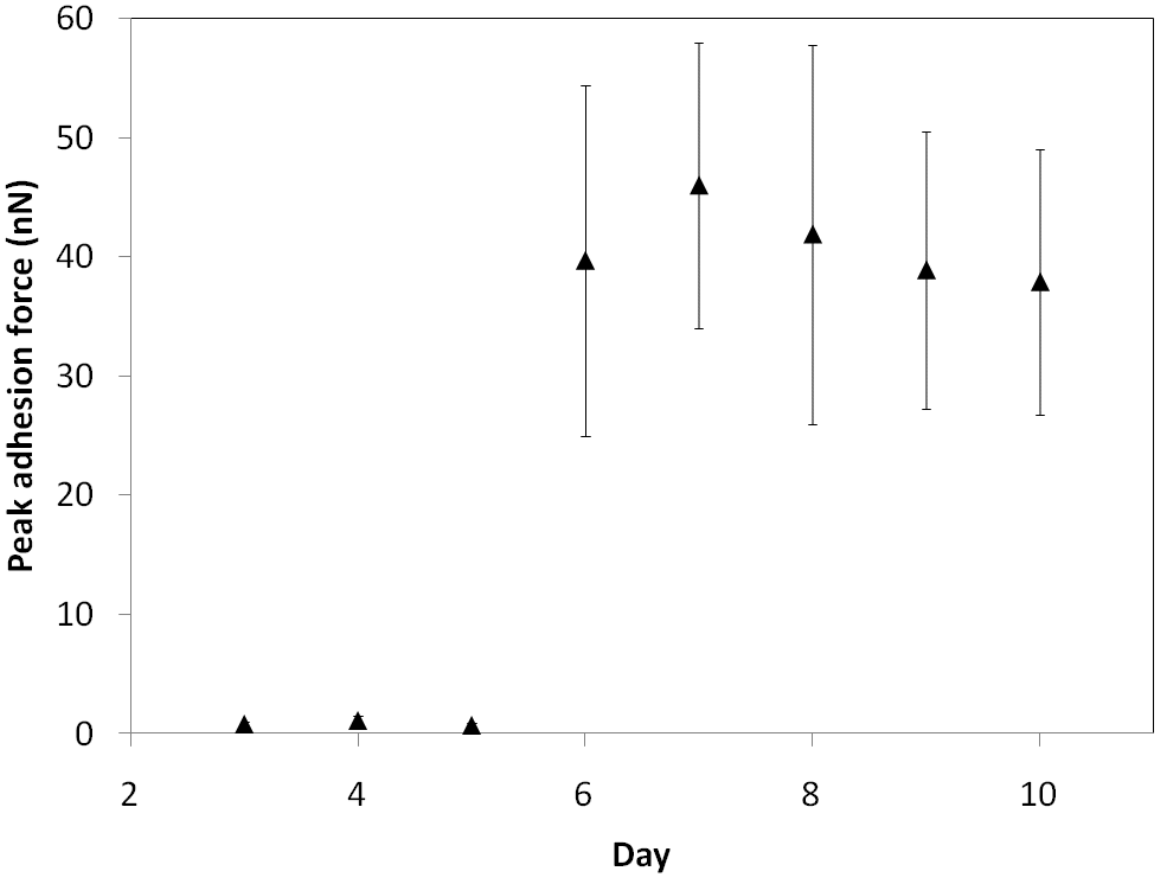

Figure 8. Typical retraction events measured using AFM for SCEBs on a) Day 3, b) Day 4, c) Day 5 B, d) Day 6 B, e) Day 7, f) Day 8, g) Day 9, h) Day 10.

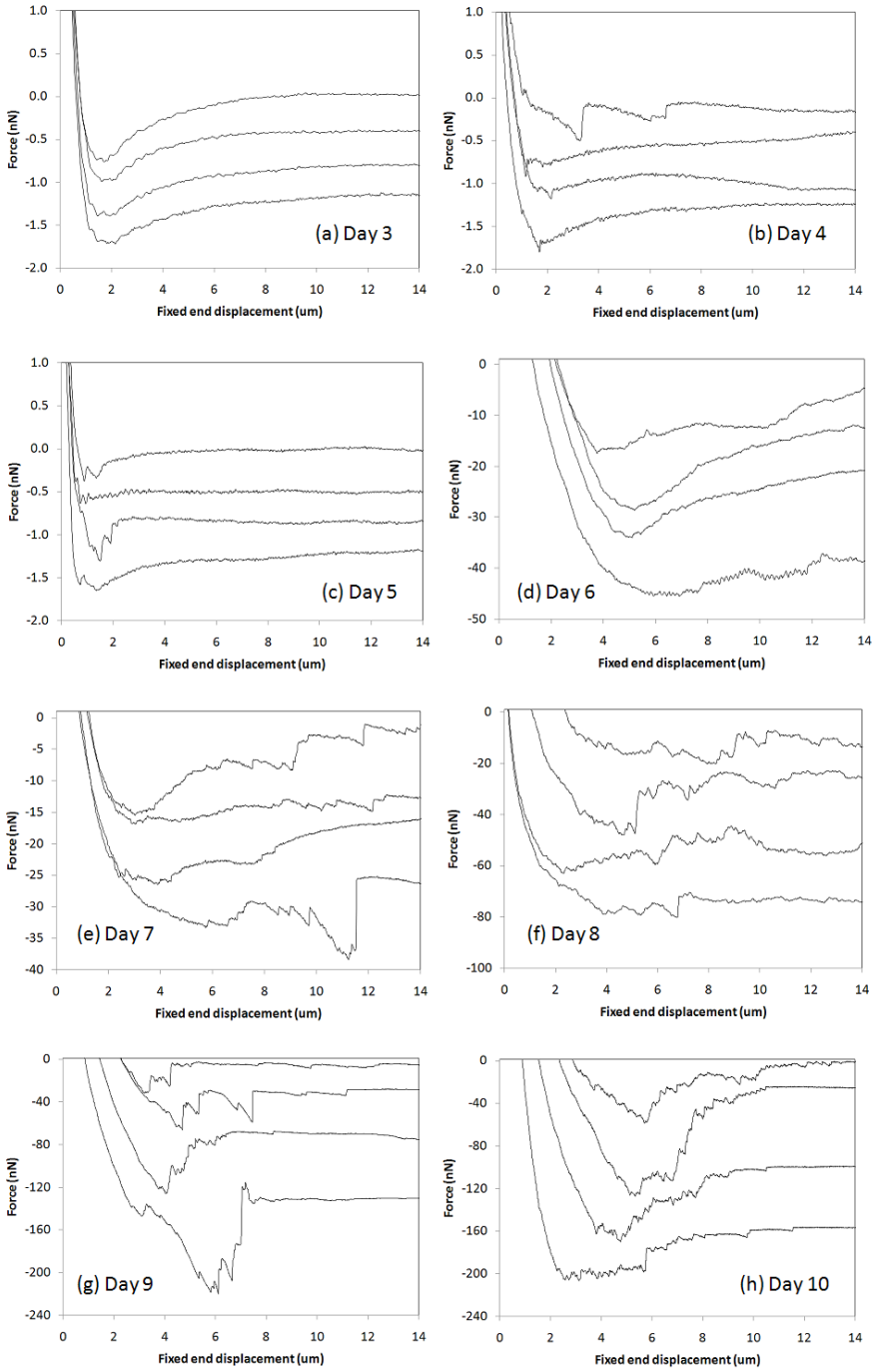

Figure 9. Distribution of peak forces measured using AFM for Day 7 natural biofilm and typical retraction data (inset). Over 1,000 measurements were performed, on three different samples.